Assessment of IDH1 Genotype and Cell Proliferation in Gliomas Using Diffusion Magnetic Resonance Imaging

Yan Xie (846348391@qq.com)
Tongji Hospital of Tongji Medical College of Huazhong University of Science and Technology
https://orcid.org/0000-0003-3608-8887
Shihui Li
Tongji Hospital of Tongji Medical College of Huazhong University of Science and Technology
Department of Radiology
Nanxi Shen
Tongji Hospital of Tongji Medical College of Huazhong University of Science and Technology
Tongjia Gan
Tongji Hospital of Tongji Medical College of Huazhong University of Science and Technology
Shun Zhang
Tongji Hospital of Tongji Medical College of Huazhong University of Science and Technology
Weiyin Vivian Liu
GE Healthcare Beijing
Wenzhen Zhu
Tongji Hospital of Tongji Medical College of Huazhong University of Science and Technology

Research Article

Keywords: diffusion magnetic resonance imaging, gliomas, Isocitrate dehydrogenase, cell proliferation

Posted Date: April 30th, 2021

DOI: https://doi.org/10.21203/rs.3.rs-468889/v1

Abstract

Purpose

To compare the efficacy of parameters from mono-, bi- and stretch-exponential diffusion weighted imaging (DWI), diffusion tensor imaging (DTI), diffusion kurtosis imaging (DKI) and neurite orientation dispersion and density imaging (NODDI) for prediction of IDH1 genotype and assessment of cell proliferation in gliomas.

Methods

91 patients with pathologically confirmed gliomas underwent DWI, multi-b-value DWI and DKI/NODDI on 3.0T MRI. The ROIs were manually placed to obtain measurements including apparent diffusion coefficient (ADC), slow ADC (D), fast ADC (D*), perfusion fraction (f), distributed diffusion coefficient (DDC), heterogeneity index (α), fractional anisotropy (FA), mean diffusivity (MD), mean kurtosis (MK), orientation dispersion index (ODI) and intracellular volume fraction (ICVF).

Results

In LrGGs, IDH1 wild-type group showed significantly lower ADC, D, f, DDC, α, MD and higher D*, MK, ODI and ICVF values than IDH1-mutant group ($P < 0.05$). Among them, α has the highest AUC value (0.846). In GBMs, no difference between IDH1-mutant and IDH1 wild-type group was found. For IDH1-mutant group, all parameters, except for FA and D*, significantly discriminated LrGGs from GBMs ($P < 0.05$). However, for IDH1 wild-type group, only ADC and DDC statistically discriminated LrGGs from GBMs ($P = 0.039$ and 0.046, respectively). In addition, MK has maximal correlation coefficient ($r = 0.612$, $P < 0.001$) and D* has the minimal correlation coefficient ($r = 0.146$, $P = 0.176$) with Ki-67 LI.

Conclusion

The α may be the most effective diffusion MRI marker for predicting IDH1 genotype in LrGGs, and MK has shown great potential in assessing glioma cell proliferation.

Introduction

In 2016, the World Health Organization (WHO) classified levels of Central Nervous System (CNS) tumors based on molecular features, specifically the isocitrate dehydrogenase 1 (IDH1) genotype [1]. IDH1 is a key enzyme involved in cellular metabolism, epigenetic regulation, redox and DNA repair, existing in the cytoplasm and peroxisomes [2]. Many studies have indicated a better prognosis of IDH1-mutant gliomas than IDH1 wild-type gliomas [3, 4]. Ye et al [5] found that IDH1 mutation causes a decrease in hypoxia-inducible factor -1α (HIF-1α), which in turn leads to the inhibition of HIF-1α-mediated biological functions

such as pro-angiogenesis, angiogenesis, migration and motility of endothelial cells. Therefore, accurate identification of glioma IDH1 genotype facilitates the formulation of treatment plans and assessment of patient prognosis.

A nuclear protein, Ki-67, represents the proliferative activity of tumors and is closely associated with tumor differentiation and infiltration [6]. The higher Ki-67 LI indicates faster tumor growth and poorer tissue differentiation. However, the cost of gene screening is high and not easy to broadly implemented [7]. To obtain tumor pathology information and Ki-67 LI via surgery or pathological biopsy is not applicable for all gliomas. Thus, an imaging approach to obtain anatomical details and tissue characteristics is essential for clinic diagnosis.

Diffusion magnetic resonance imaging (dMRI) is a non-invasive method to reflect microstructure information of diffusion of water molecules. The conventional mono-exponential diffusion-weighted imaging (DWI) reflects water motion paths *in vivo*. Diffusion tensor imaging (DTI) indicates the integrity of the white matter fiber tracts in the brain under the assumption of water random movements in Gaussian distribution [8]. Since the complex cellular microenvironment in real organisms is limited by organelles, cell membranes and extracellular gaps [9, 10], water moves in non-Gaussian distribution and can be revealed by diffusion kurtosis imaging (DKI) [11]. DKI cannot reflect the intrinsic biophysical mechanisms such as the altered membrane permeability of axons, while neurite orientation dispersion and density imaging (NODDI) reflects a closer approximation to the real diffusion pattern of water molecules in the tissue microenvironment via characterizing the three main tissue cavities in the microstructural environment, namely, restricted diffusion of water within the neurite, hindered diffusion of water outside the neurite, and free diffusion of water in the cerebrospinal fluid [12]. In addition, the bi-exponential intravoxel incoherent motion (IVIM) imaging is able to separate the slow diffusive motion in response to intra- and extracellular water molecules as intra-tissue diffusion from the fast diffusive motion in response to intravascular water molecules as vascular perfusion [13], while the stretch-exponential DWI is able to describe the tissue heterogeneity and the continuous distribution of water molecules in the microstructure [14].

dMRI analyzed with different diffusion models reflects the complexity of tumor microstructure. Till now, few studies have been performed to compare the efficacy of these diffusion models in terms of IDH1 genotype. The purpose of this study was to assess IDH1 genotype and cell proliferation using mono-exponential, bi-exponential, stretch-exponential DWI, DTI, DKI and NODDI models.

Materials And Methods

Patient Population

This study was approved by local ethics committee and written informed consent was waived due to the retrospective study design. Patients were included in the study if they met the following inclusion criteria: (a) pathologically confirmed primary gliomas; (b) preoperative DWI, multi-b-value DWI, and DKI/NODDI acquisition were performed; (c) IDH1 genotype measured by genetic screening or immunohistochemistry

was available. The following were exclusion criteria: (a) purely cystic gliomas; (b) lack of routine MRI images. From July 2017 to December 2020, a total of 94 patients meeting the above inclusion criteria were enrolled in the study. Two cases with purely cystic glioma and one lack of routine images were excluded. In total, 91 patients were recruited into this study.

Image Data Acquisition

All MR images were performed on the a 3T MR system (Discovery MR750, GE Medical Systems, Milwaukee, WI, USA) with a 32-channel head coil. Routine axial sequences include T1 fluid-attenuated inversion recovery (T1 FLAIR), T2 fast spin echo (T2 FSE) and T2 fluid-attenuated inversion recovery (T2 FLAIR).

Three diffusion imaging data were obtained using spin-echo echo-planar imaging (SE-EPI) sequences before the injection of contrast agents. The parameters of DWI are as follows: TR/TE = 3000/70 ms, NEX = 1, matrix =160×160, slice thickness = 5 mm, slice spacing = 1.5 mm, FOV = 240×240 mm^2, b = 0, 1000s/mm^2, and acquisition time was 42 s. Multi-b-value DWI was performed with 20 b values (b = 0, 20, 50, 80, 100, 150, 200, 400, 600, 800, 1000, 1200, 1500, 2000, 2400, 2800, 3200, 3600, 4000 and 4500 s/mm^2), TR/TE=3200/90.6 ms, matrix=160×160, slice thickness = 5 mm, spacing = 1.5 mm, FOV=240×240 mm^2, acquisition time was 5 min 52 s. DKI/NODDI was performed with 3 b values (b = 0, 1250, 2500 s/mm^2) and 25 uniformly distributed directions for each nonzero b-value, TR/TE = 6500/85, NEX = 1, matrix = 128×128, slice thickness = 3 mm, spacing = 0 mm, FOV = 240×240 mm^2, acquisition time was 5 min 45 s.

Image Processing and Regions of Interest Analysis

Mono-, bi- and stretch-exponential DWI, IVIM, DTI, DKI parametric maps were processed using GE Advantage workstation (version 4.5). After brain extraction of images by MRIcron (Version 12 12 2012), the NODDI parametric maps was processed using a MATLAB toolbox (https://www.nitrc.org/projects/noddi_toolbox). The formulas of each dMRI model are in Online Resource 1.

All parametric maps and routine MR images were analyzed using ImageJ software (version 1.52a, NIH, USA). Before drawing the regions of interest (ROIs), the size (256×256), number of slices (43) as well as canvas size (240×240mm^2) of T1-FLAIR, T2 FSE and all parameter maps were adjusted to ensure they had the same image resolution, number of slices and FOV. Referring to T1-FLAIR and T2 FSE, regions of interest (ROIs) (range, 25-38 pixels, mean size = 32.516 pixels) were placed on the tumor parenchyma with the lowest mean signal intensity in ADC maps to avoid hemorrhage, calcification, edema, necrosis and cystic lesions. Then, the ROIs on ADC maps were matched to other parameter maps to obtain measurements for each patient.

Statistical Analysis

For demographic characteristics, chi-square tests or R × C columnar tables and independent sample t-tests were respectively used to test categorical variables and continuous variables. Interobserver agreement was evaluated by intraclass correlation coefficient (ICC). Mann-Whitney U test was used to compare the differences of all parameters between glioma subtypes. Receiver operating characteristic (ROC) curves were performed to evaluate the diagnostic efficacy of each parameter. And area under the curve (AUC) was compared by Z test. The correlation between each parameter and proliferation index was calculated by Spearman correlation analysis. All statistical analyses were performed with SPSS (Version 19.0.0, IBM, Armonk, NY, USA) and MedCalc (Version 15.8, MedCalc Software, Acacialaan, Ostend, Belgium). $P < 0.05$ was considered to exist statistical significance.

Results

Patient characteristics and demographics

In this study, there were 42 patients with IDH1-mutant glioma and 49 patients with IDH1 wild-type glioma. Patients with IDH1-mutant glioma (43.2±12.3 years) were younger than those with IDH1 wild-type glioma (50.2±12.2 years) (P=0.008). There was a significant difference of pathological grade distribution between IDH1-mutant group and IDH1 wild-type group (P<0.001) (Table 1).

Interobserver Agreement

The interobserver agreement for DDC value was the highest (ICC: 0.970, P<0.001) and for D* value was the lowest (ICC: 0.533, P=0.001). The interobserver agreement was also generally good for the ADC, D, f, α, MD, MK, D, f and ICVF values (ICCs range 0.845-0.960, P<0.001). In addition, the inter-observer agreement for FA and ODI value were relatively lower (ICC: 0.612, P<0.001; and 0.748, P<0.001, respectively) (Online Resource 2).

Correlation of dMRI parameters with IDH1 genotype and grade

Fig. 1 shows the enhanced T1WI and dMRI parameter maps of typical IDH1-mutant and IDH1 wild-type glioma patients. In LrGGs, IDH1 wild-type group showed significantly lower ADC, D, f, DDC, α, and MD values (P<0.05) and higher D*, MK, ODI and ICVF values (P <0.05) than IDH1-mutant group. However, there was no significant difference in FA value (P=0.827) between the two groups (Fig. 2). The AUC values for ADC, D, f, DDC, α, MD and ICVF were significantly greater than that for FA in the differentiation of IDH1-mutant and wild-type groups (P <0.05). α had the highest AUC value which was significantly higher than that of D*(0.846 vs 0.696, P <0.05) (Fig. 3). For GBMs, no significant difference of these parameters was found between IDH1-mutant and IDH1 wild-type groups.

The comparison and ROC results of each parameter for distinguishing LrGGs and GBMs in the presence of the same IDH1 genotype was showed in Online Resource 3. In IDH1-mutant group, all parameters of dMRI, except FA and D*, can significantly distinguish LrGGs from GBMs (P<0.05) with the AUC values (range 0.794-0.916); among them, MK had the largest AUC value. In IDH1 wild-type group, only ADC and

DDC were statistically different between LrGGs and GBMs (P=0.039 and P=0.046, respectively), with lower AUC values (0.686 and 0.680, respectively).

Correlation between dMRI parameters and cell proliferation index

The expression of Ki-67 LI was detected by immunohistochemical staining in 87 patients in this study. Fig. 4 shows the Spearman correlation between Ki-67 LI and dMRI parameters in gliomas. Significant positive correlation was found between Ki-67 LI and MK (r = 0.612, P < 0.001), ODI (r = 0.264, P = 0.014) as well as ICVF (r =0.605, P < 0.001). In contrast, ADC, D, f, DDC, α and MD showed a significant negative correlation with Ki-67 LI (r = -0.561, P < 0.001; r = -0.594, P < 0.001; r = -0.524, P < 0.001; r = -0.576, P < 0.001; r = -0.499, P < 0.001; r = -0.599, P < 0.001, respectively). FA and D* had no significant correlation with Ki-67 LI (r = 0.182, P = 0.092; r = 0.146, P=0.176, respectively). MK has the maximal correlation coefficient and D* has the minimal.

Discussion

Our study showed dMRI is potentially valuable for prediction of IDH1 genotype in LrGGs, where α is the most effective predictor of IDH1 mutation status. Also, dMRI parameters are promising in the assessment of cell proliferation, especially maximal correlation coefficient was found between MK and proliferation index.

Radiological differences were found between IDH1-mutant and wild-type groups in LrGGs. We suspected that IDH1 wild type existed in the LrGGs when more complex organizational structure, more abundant microvasculature, higher cell density and more diffusion barriers appeared. However, none of the parameters showed significant differences in the identification of IDH1-mutant and wild-type groups in GBMs due to a single parameter with insufficient ability to discriminating diffusion and perfusion patterns of highly malignant and structurally complex. This hints us to further explore differences in the GBM groups using a combination of multiple parameters in the future.

Previous studies have demonstrated the ability of conventional DWI and DTI to distinguish IDH-mutant gliomas from IDH wild-type gliomas[15, 16]. In our study, ADC and MD values of IDH1 wild-type group were significantly lower than that of IDH1-mutant group in LrGGs. FA showed ineffective prediction on IDH1 genotype, possibly due to the high heterogeneity in FA values for the solid component of the tumor, which is consistent with the results of Tan et al [17].

Many studies have found that DKI has better efficacy in identifying molecular subtypes of gliomas [18, 19]. A DKI parameter MK reflects the complexity of the tissue microenvironment under the assumption of non-Gaussian distribution in the organism. Similar to the results reported by Zhao et al [20], our finding showed MK effectively discriminated IDH1-mutant group from wild-type group in LrGGs.

ODI and ICVF computed based on the NODDI model represent neurite dispersion characteristics and neurite density, respectively. Since both neuronal density and directional dispersion affect FA value [21],

our results showed both ODI and ICVF significantly distinguished IDH1-mutant group from IDH1 wild-type group in LrGGs. IDH1 wild-type gliomas may be more proliferative and aggressive due to more complex microstructure and higher dispersion of neurites and thus possess higher ODI and ICVF values. Zhao et al. [22] reported that the mean ICVF was significantly higher in GBMs with IDH1 mutation than that without IDH1 mutation. However, only 4 cases of IDH1-mutant GBMs were collected in their study, the findings still need to be confirmed even different to ours.

The IVIM model was proposed by Le Bihan et al [23], where D represents the diffusion movement of water molecules inside and outside the cell, D* reflects the blood perfusion of the microcirculation, and f represents the abundance of capillaries in the tissue. In the current study, the performance of D was slightly better than that of ADC in identifying the mutation status of IDH1 genotype in LrGGs perhaps due to D eliminates the influence of perfusion and more accurately reflects the diffusion and movement of water molecules. The D* value of IDH1 wild-type group is higher than that of IDH1-mutant group in LrGGs, indicating that IDH1 wild-type glioma has more abundant blood perfusion. However, interobserver agreement and the AUC value of D* was low even it had significant difference in the identification of IDH1 mutation status in LrGGs. The instability of the parameters may lead to a limited application of D* in glioma IDH1 genotype prediction. Furthermore, f value is higher in IDH1mutant gliomas, inconsistent with Wang et al [24]. The same contradictory results exist in studies of glioma grading, where f values are higher in low-grade gliomas than in high-grade gliomas [25]. Le Bihan et al. [26] suggested that the IVIM model is sensitive to fluid flow distributed within any voxel, not just blood flow. More relatively unrestricted water molecules outside the IDH1-mutant glioma cells may have contributed to the increase of f values. Alternatively, these differences may be due to different IVIM model parameters, fitting methods, and ROI plotting methods [27].

The stretched-exponential DWI model showed excellent efficacy in IDH1 genotype discrimination in our study, and α was able to distinguish IDH1 mutation status in LrGGs with the largest AUC value and high sensitivity and specificity. Lower α values indicate that the diffusion of water molecules in the tissue was inhomogeneous, and the heterogeneity of the tissue was higher[28]. We speculate that the microenvironment of IDH1 wild-type glioma is more complicated, such as cell swelling and vascular proliferation, so it exhibits greater heterogeneity of intra-voxel diffusion.

In this study, the six diffusion models all provide at least one parameter with effective prediction performance on the IDH1 genotype of LrGGs. This is of great clinical importance for the prediction of IDH1 wild-type LrGGs, which have a malignant clinical course despite being pathologically relatively inert alterations. Therefore, accurate and non-invasive prediction of the IDH1 genotype in LrGGs allows for timely treatment planning to impede malignant transformation of the disease.

We also investigated the prediction of glioma grading by dMRI under the same IDH1 genotype. Generally speaking, high-grade gliomas tend to be more heterogeneous, as our findings. However, IDH1 wild-type LrGGs and GBMs showed only statistically different ADC and DDC. Some studies have found that even in patients with IDH wild-type LrGG, tumors exhibit high levels of aggressiveness, with overall survival times

similar to those of IDH wild-type GBM[29, 30]. This may explain our results, probably because the similar high heterogeneity and aggressiveness of IDH1 wild-type gliomas, resulting in most parameters that do not differ significantly between LrGGs and GBMs both with wild-type IDH1. In a word, with the increase of pathological grade, the tumor microstructure is more complex, with higher cell density and more disturbed water molecule movement, but IDH1 gene phenotype will affect the development of gliomas at a microscopic point of view. Compared with previous pathological grading studies[28], our study combined the pathological grading of gliomas with molecular phenotypes, which contributes to a more comprehensive understanding of the characteristics and microstructure of gliomas.

Nuclear protein Ki-67 is associated with cell proliferation specifically expressed in tumor cells [31, 32]. As the malignancy of the tumor increases, the blood supply becomes more abundant, the number of cells increases, malignant biological behavior ensues, such as hemorrhage and necrosis, and neovascularization forms further [33, 34]. And these aforementioned alterations can affect the complexity and heterogeneity of tumor microstructure, when cellular gaps are smaller, water molecules diffusion is more restricted and movement is more disturbed. Zhang et al. [35] found MK and D have considerable potential to predict the degree of proliferation in diffuse astrocytomas. This is similar to our findings, where MK has maximal correlation coefficient with cell proliferation index. However, no significant correlation was found between FA and Ki-67 LI, which may be because the level of cell proliferation in response to Ki-67 only affects the size of the diffusion and not the pattern of diffusion routes. No significant correlation was also found between D* and Ki-67 LI. We speculate that D* reflects more perfusion-related information and is not sensitive enough to changes in cell proliferation.

Our study had some limitations. First, the sample size of this study was small and it was a single-center study. Future multicenter studies with large sample sizes are needed to validate the results of this study. Secondly, only one molecule, IDH1, was considered in this study, but many other molecules status such as 1p/19q codeletion and O6-methylguanine-DNA methyltransferase promoter methylation also play an important role in the development of gliomas, which needs to be further investigated. Finally, we performed 2D ROI placement at the tumor parenchyma site with the lowest ADC value, which may ignore the overall tumor condition.

Conclusion

α may be the most promising dMRI marker for predicting IDH1 mutation status in LrGGs, and MK may be the most potential dMRI marker in assessing cell proliferation. The dMRI can effectively reflect microstructural changes caused by molecular differences and provide useful additional information for clinical treatment.

Acknowledgements

Contract grant sponsor: National Natural Science Foundation of China; contract grant number: 81730049.

References

1. Karsy M, Guan J, Cohen AL, Jensen RL, Colman H (2017) New Molecular Considerations for Glioma: IDH, ATRX, BRAF, TERT, H3 K27M. Current neurology and neuroscience reports 17: 19 doi:10.1007/s11910-017-0722-5
2. Fu Y, Huang R, Du J, Yang R, An N, Liang A (2010) Glioma-derived mutations in IDH: from mechanism to potential therapy. Biochemical and biophysical research communications 397: 127-130 doi:10.1016/j.bbrc.2010.05.115
3. Turkalp Z, Karamchandani J, Das S (2014) IDH mutation in glioma: new insights and promises for the future. JAMA neurology 71: 1319-1325 doi:10.1001/jamaneurol.2014.1205
4. Shen G, Wang R, Gao B, Zhang Z, Wu G, Pope W (2020) The MRI Features and Prognosis of Gliomas Associated With IDH1 Mutation: A Single Center Study in Southwest China. Front Oncol 10: 852 doi:10.3389/fonc.2020.00852
5. Ye D, Ma S, Xiong Y, Guan KL (2013) R-2-hydroxyglutarate as the key effector of IDH mutations promoting oncogenesis. Cancer Cell 23: 274-276 doi:10.1016/j.ccr.2013.03.005
6. Habberstad AH, Gulati S, Torp SH (2011) Evaluation of the proliferation markers Ki-67/MIB-1, mitosin, survivin, pHH3, and DNA topoisomerase IIalpha in human anaplastic astrocytomas--an immunohistochemical study. Diagn Pathol 6: 43 doi:10.1186/1746-1596-6-43
7. Jiang S, Rui Q, Wang Y, Heo HY, Zou T, Yu H, Zhang Y, Wang X, Du Y, Wen X, Chen F, Wang J, Eberhart CG, Zhou J, Wen Z (2018) Discriminating MGMT promoter methylation status in patients with glioblastoma employing amide proton transfer-weighted MRI metrics. Eur Radiol 28: 2115-2123 doi:10.1007/s00330-017-5182-4
8. Maier SE, Sun Y, Mulkern RV (2010) Diffusion imaging of brain tumors. NMR in biomedicine 23: 849-864 doi:10.1002/nbm.1544
9. Van Cauter S, Veraart J, Sijbers J, Peeters RR, Himmelreich U, De Keyzer F, Van Gool SW, Van Calenbergh F, De Vleeschouwer S, Van Hecke W, Sunaert S (2012) Gliomas: diffusion kurtosis MR imaging in grading. Radiology 263: 492-501 doi:10.1148/radiol.12110927
10. Jiang R, Jiang J, Zhao L, Zhang J, Zhang S, Yao Y, Yang S, Shi J, Shen N, Su C, Zhang J, Zhu W (2015) Diffusion kurtosis imaging can efficiently assess the glioma grade and cellular proliferation. Oncotarget 6: 42380-42393 doi:10.18632/oncotarget.5675
11. Wu EX, Cheung MM (2010) MR diffusion kurtosis imaging for neural tissue characterization. NMR in biomedicine 23: 836-848 doi:10.1002/nbm.1506
12. Zhang H, Schneider T, Wheeler-Kingshott CA, Alexander DC (2012) NODDI: practical in vivo neurite orientation dispersion and density imaging of the human brain. Neuroimage 61: 1000-1016 doi:10.1016/j.neuroimage.2012.03.072
13. Shen N, Zhao L, Jiang J, Jiang R, Su C, Zhang S, Tang X, Zhu W (2016) Intravoxel incoherent motion diffusion-weighted imaging analysis of diffusion and microperfusion in grading gliomas and

comparison with arterial spin labeling for evaluation of tumor perfusion. J Magn Reson Imaging 44: 620-632 doi:10.1002/jmri.25191

14. Bennett KM, Schmainda KM, Bennett RT, Rowe DB, Lu H, Hyde JS (2003) Characterization of continuously distributed cortical water diffusion rates with a stretched-exponential model. Magn Reson Med 50: 727-734 doi:10.1002/mrm.10581
15. Wu CC, Jain R, Radmanesh A, Poisson LM, Guo WY, Zagzag D, Snuderl M, Placantonakis DG, Golfinos J, Chi AS (2018) Predicting Genotype and Survival in Glioma Using Standard Clinical MR Imaging Apparent Diffusion Coefficient Images: A Pilot Study from The Cancer Genome Atlas. AJNR American journal of neuroradiology 39: 1814-1820 doi:10.3174/ajnr.A5794
16. Xiong J, Tan W, Wen J, Pan J, Wang Y, Zhang J, Geng D (2016) Combination of diffusion tensor imaging and conventional MRI correlates with isocitrate dehydrogenase 1/2 mutations but not 1p/19q genotyping in oligodendroglial tumours. Eur Radiol 26: 1705-1715 doi:10.1007/s00330-015-4025-4
17. Tan Y, Zhang H, Wang X, Qin J, Wang L, Yang G, Yan H (2019) Comparing the value of DKI and DTI in detecting isocitrate dehydrogenase genotype of astrocytomas. Clinical radiology 74: 314-320 doi:10.1016/j.crad.2018.12.004
18. Hempel J-M, Bisdas S, Schittenhelm J, Brendle C, Bender B, Wassmann H, Skardelly M, Tabatabai G, Vega SC, Ernemann U, Klose U (2016) In vivo molecular profiling of human glioma using diffusion kurtosis imaging. Journal of Neuro-Oncology 131: 93-101 doi:10.1007/s11060-016-2272-0
19. Hempel JM, Schittenhelm J, Brendle C, Bender B, Bier G, Skardelly M, Tabatabai G, Castaneda Vega S, Ernemann U, Klose U (2017) Histogram analysis of diffusion kurtosis imaging estimates for in vivo assessment of 2016 WHO glioma grades: A cross-sectional observational study. Eur J Radiol 95: 202-211 doi:10.1016/j.ejrad.2017.08.008
20. Zhao J, Wang YL, Li XB, Hu MS, Li ZH, Song YK, Wang JY, Tian YS, Liu DW, Yan X, Jiang L, Yang ZY, Chu JP (2019) Comparative analysis of the diffusion kurtosis imaging and diffusion tensor imaging in grading gliomas, predicting tumour cell proliferation and IDH-1 gene mutation status. J Neurooncol 141: 195-203 doi:10.1007/s11060-018-03025-7
21. Li SH, Jiang RF, Zhang J, Su CL, Chen XW, Zhang JX, Jiang JJ, Zhu WZ (2019) Application of Neurite Orientation Dispersion and Density Imaging in Assessing Glioma Grades and Cellular Proliferation. World neurosurgery 131: e247-e254 doi:10.1016/j.wneu.2019.07.121
22. Zhao J, Li JB, Wang JY, Wang YL, Liu DW, Li XB, Song YK, Tian YS, Yan X, Li ZH, He SF, Huang XL, Jiang L, Yang ZY, Chu JP (2018) Quantitative analysis of neurite orientation dispersion and density imaging in grading gliomas and detecting IDH-1 gene mutation status. Neuroimage Clin 19: 174-181 doi:10.1016/j.nicl.2018.04.011
23. Le Bihan D, Breton E, Lallemand D, Grenier P, Cabanis E, Laval-Jeantet M (1986) MR imaging of intravoxel incoherent motions: application to diffusion and perfusion in neurologic disorders. Radiology 161: 401-407 doi:10.1148/radiology.161.2.3763909

24. Wang X, Chen XZ, Shi L, Dai JP (2019) Glioma grading and IDH1 mutational status: assessment by intravoxel incoherent motion MRI. Clinical radiology 74: 651 e657-651 e614 doi:10.1016/j.crad.2019.03.020
25. Hu YC, Yan LF, Wu L, Du P, Chen BY, Wang L, Wang SM, Han Y, Tian Q, Yu Y, Xu TY, Wang W, Cui GB (2014) Intravoxel incoherent motion diffusion-weighted MR imaging of gliomas: efficacy in preoperative grading. Sci Rep 4: 7208 doi:10.1038/srep07208
26. Le Bihan D (2019) What can we see with IVIM MRI? Neuroimage 187: 56-67 doi:10.1016/j.neuroimage.2017.12.062
27. Cho GY, Moy L, Zhang JL, Baete S, Lattanzi R, Moccaldi M, Babb JS, Kim S, Sodickson DK, Sigmund EE (2015) Comparison of fitting methods and b-value sampling strategies for intravoxel incoherent motion in breast cancer. Magn Reson Med 74: 1077-1085 doi:10.1002/mrm.25484
28. Bai. Y, Lin. Y, Tian. J, Shi. D, Cheng. J, Haacke. EM, Hong. X, Ma. B, Zhou. J, Wang. M (2016) grading of gliomas by Using Monoexponential, Biexponential, and stretched exponential Diffusion-weighted Mr imaging and Diffusion Kurtosis Mr imaging. Radiology 278: 496-504
29. Wijnenga MMJ, Dubbink HJ, French PJ, Synhaeve NE, Dinjens WNM, Atmodimedjo PN, Kros JM, Dirven CMF, Vincent A, van den Bent MJ (2017) Molecular and clinical heterogeneity of adult diffuse low-grade IDH wild-type gliomas: assessment of TERT promoter mutation and chromosome 7 and 10 copy number status allows superior prognostic stratification. Acta Neuropathol 134: 957-959 doi:10.1007/s00401-017-1781-z
30. Eckel-Passow JE, Lachance DH, Molinaro AM, Walsh KM, Decker PA, Sicotte H, Pekmezci M, Rice T, Kosel ML, Smirnov IV, Sarkar G, Caron AA, Kollmeyer TM, Praska CE, Chada AR, Halder C, Hansen HM, McCoy LS, Bracci PM, Marshall R, Zheng S, Reis GF, Pico AR, O'Neill BP, Buckner JC, Giannini C, Huse JT, Perry A, Tihan T, Berger MS, Chang SM, Prados MD, Wiemels J, Wiencke JK, Wrensch MR, Jenkins RB (2015) Glioma Groups Based on 1p/19q, IDH, and TERT Promoter Mutations in Tumors. N Engl J Med 372: 2499-2508 doi:10.1056/NEJMoa1407279
31. Alexiou GA, Tsiouris S, Kyritsis AP, Argyropoulou MI, Voulgaris S, Fotopoulos AD (2010) Assessment of glioma proliferation using imaging modalities. Journal of clinical neuroscience : official journal of the Neurosurgical Society of Australasia 17: 1233-1238 doi:10.1016/j.jocn.2010.03.021
32. Gates EDH, Lin JS, Weinberg JS, Hamilton J, Prabhu SS, Hazle JD, Fuller GN, Baladandayuthapani V, Fuentes D, Schellingerhout D (2019) Guiding the first biopsy in glioma patients using estimated Ki-67 maps derived from MRI: conventional versus advanced imaging. Neuro Oncol 21: 527-536 doi:10.1093/neuonc/noz004
33. Tietze A, Hansen MB, Østergaard L, Jespersen SN, Sangill R, Lund TE, Geneser M, Hjelm M, Hansen B (2015) Mean Diffusional Kurtosis in Patients with Glioma: Initial Results with a Fast Imaging Method in a Clinical Setting. AJNR American journal of neuroradiology 36: 1472-1478 doi:10.3174/ajnr.A4311
34. Raab P, Hattingen E, Franz K, Zanella FE, Lanfermann H (2010) Cerebral gliomas: diffusional kurtosis imaging analysis of microstructural differences. Radiology 254: 876-881

doi:10.1148/radiol.09090819

35. Zhang J, Chen X, Chen D, Wang Z, Li S, Zhu W (2018) Grading and proliferation assessment of diffuse astrocytic tumors with monoexponential, biexponential, and stretched-exponential diffusion-weighted imaging and diffusion kurtosis imaging. Eur J Radiol 109: 188-195 doi:10.1016/j.ejrad.2018.11.003

Declarations

Funding This work was supported by National Natural Science Foundation of China (Grant number:81730049).

Conflicts of interest The authors have no financial or proprietary interests in any material discussed in this article.

Availability of data and material The datasets used or analysed during the current study are available from the corresponding author on reasonable request.

Code availability Not applicable

Authors' contributions Yan Xie and Shihui Li conceived and designed the study. Yan Xie and Tongjia Gan performed the experiments. Yan Xie wrote the paper. Shihui Li, Nanxi Shen, Shun Zhang, Weiyin Vivian Liu and Wenzhen Zhu reviewed and edited the manuscript. All authors read and approved the manuscript.

Ethics approval This study was approved by the Ethics Committee of Tongji Hospital of Huazhong University of Science and Technology and abided by the statement of ethical standards.

Consent to participate The written informed consent was waived due to the retrospective study design.

Consent for publication Additional informed consent was waived from all individual participants due to anonymous patient data.

Tables

Table 1 Patient characteristics and demographics

Characteristics	IDH1-Mut	IDH1-WT	P-value
No. of patients	42	49	NA
Age (mean±SD, years)	43.2±12.3	50.2±12.2	0.008**
Sex (F/M)	22/20	21/28	0.405
Pathological grading (II/ III/ IV)	19/13/10	8/7/34	<0.001***

Note: ∗∗ = P< 0.01, ∗∗∗ = P<0.001. F, female; M, male; Mut, mutant; WT, wild-type. NA, not applicable.

Figures

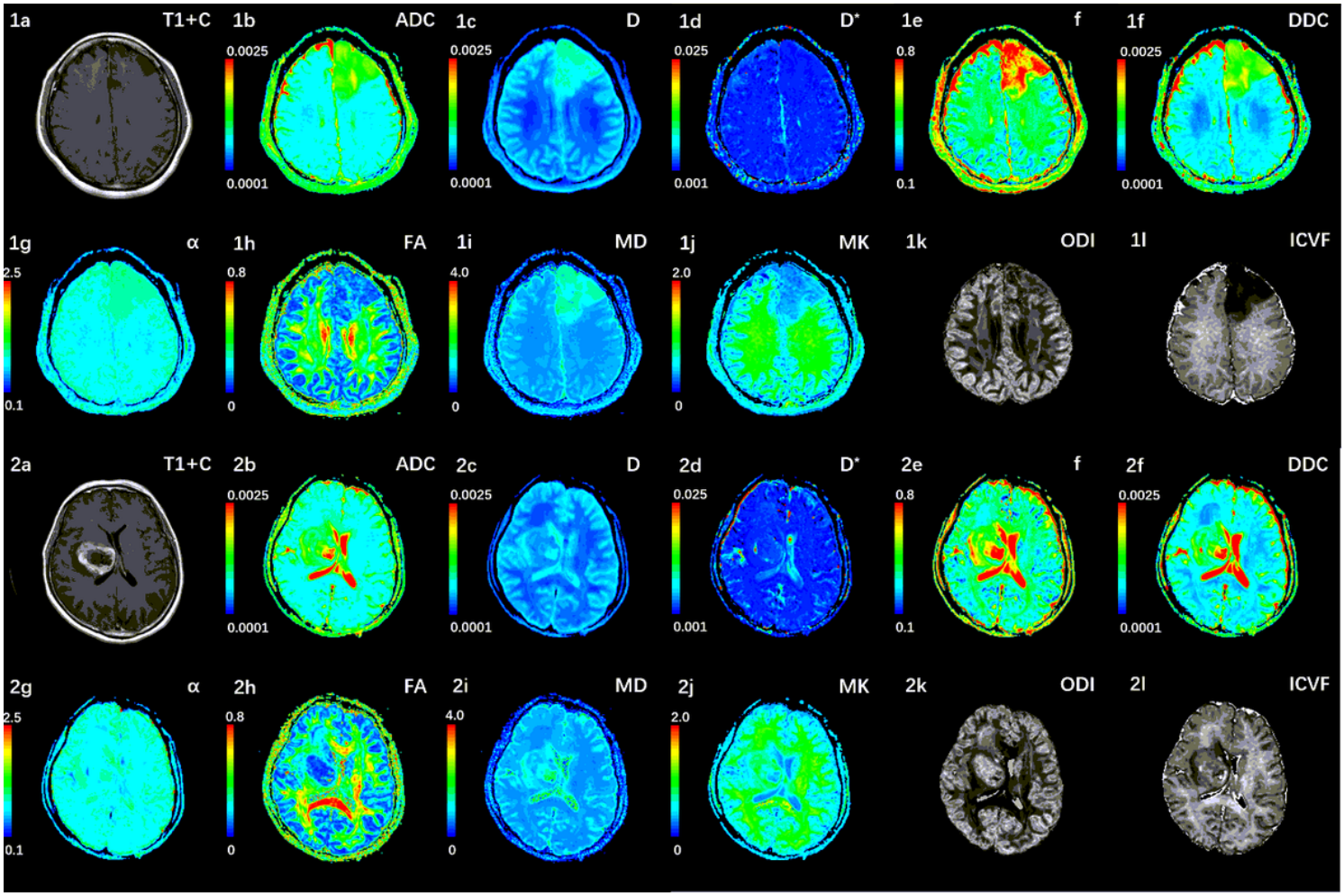

Figure 1

Images 1a–1l correspond to a 38-year-old female with a IDH1-mutant grade III glioma in the left frontal lobe. The ADC, MD, D, f, and DDC, as well as α maps show increased values in the solid part of the tumor, while D*, MK, ODI and ICVF maps show decreased values. Images 2a–2l correspond to a 59-year-old female with a IDH1 wild-type grade III glioma in the right basal ganglia. The ADC, MD, D, f, and DDC, as well as α maps show decreased values in the solid part of the tumor, while D*, MK, ODI and ICVF maps show increased values. ADC, D, D*, and DDC as well as MD are in units of 10-3 mm2/sec.

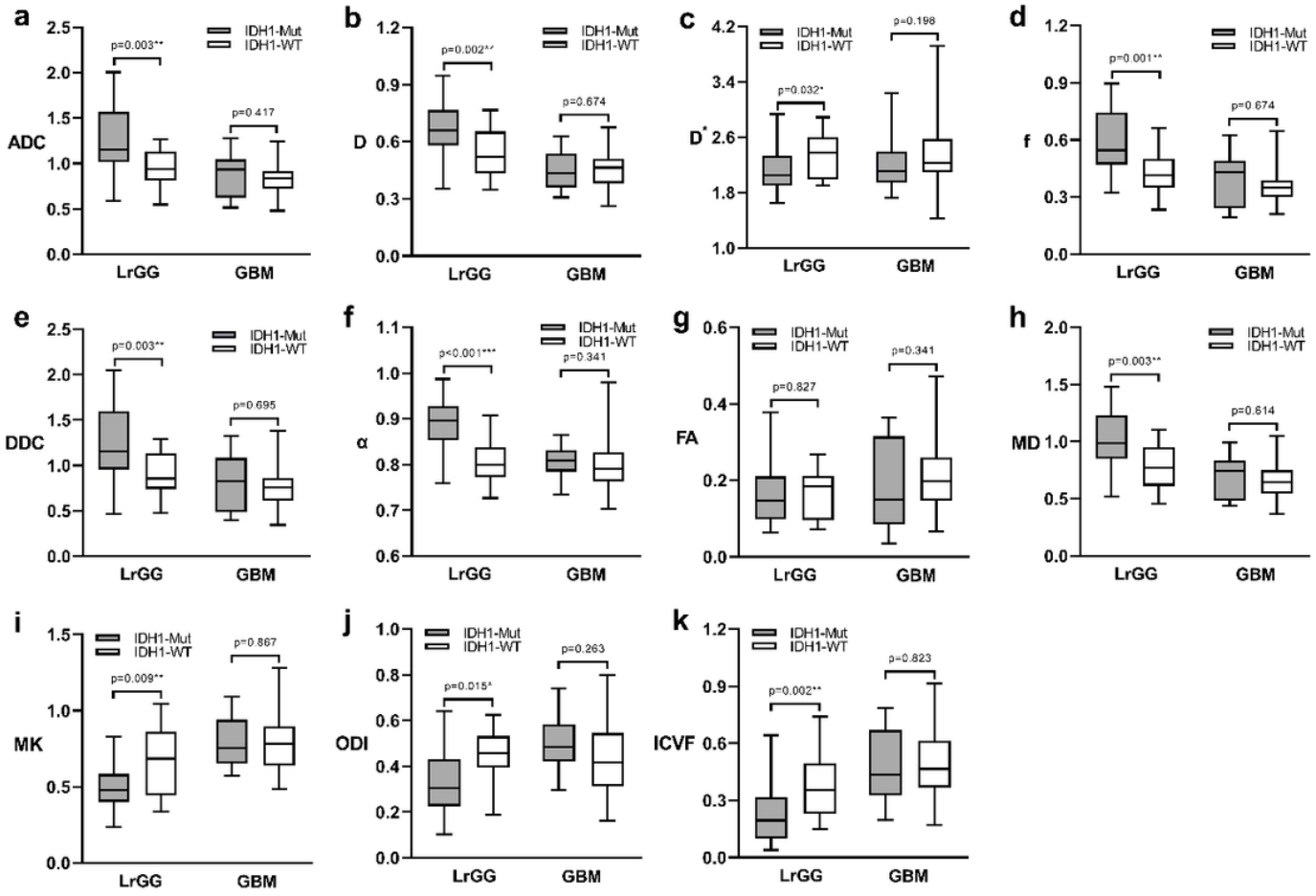

Figure 2

Box and whisker plots of dMRI-derived parameter in LrGGs and GBMs stratified according to IDH1 genotype. Boxes represent the median ± quartiles, with whiskers extending to the maximum and minimum values. ADC, D, D*, and DDC as well as MD are in units of 10-3 mm2/sec. ∗ = P<0.05, ∗∗ = P< 0.01, ∗∗∗ = P<0.001. Mut, mutant; WT, wild-type; LrGG, lower-grade glioma; GBM, glioblastoma.

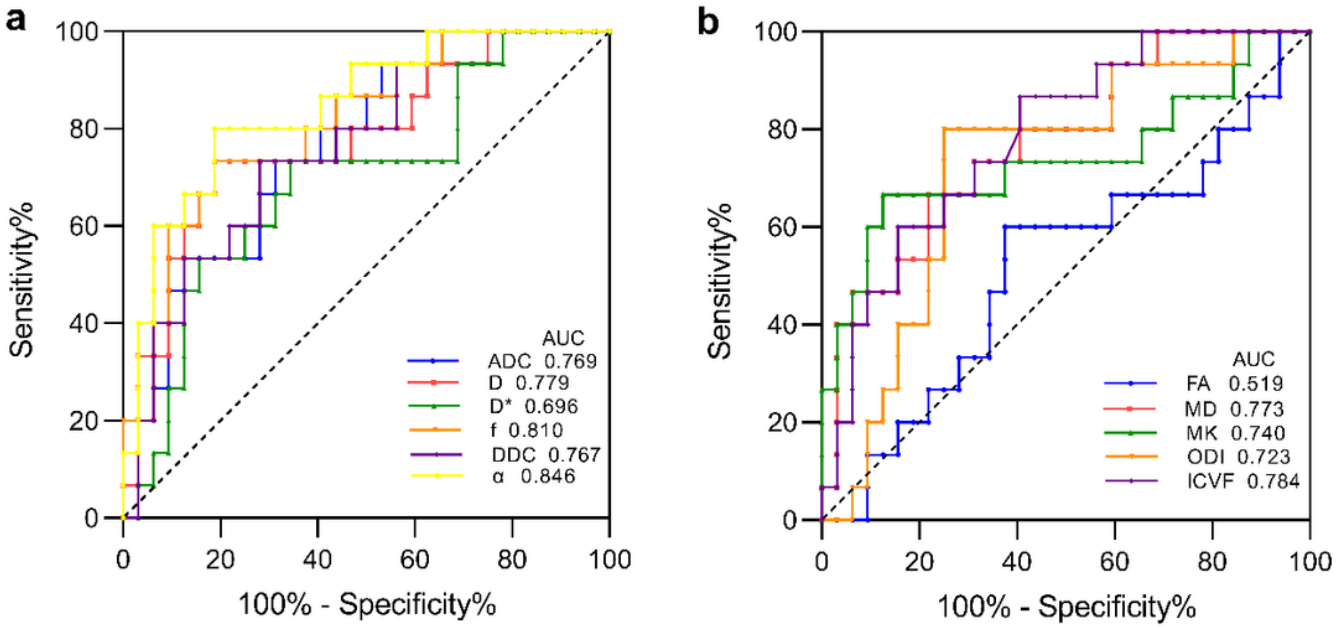

Figure 3

ROC curves of each parameter for distinguishing mutant and wild-type IDH1 in LrGGs.

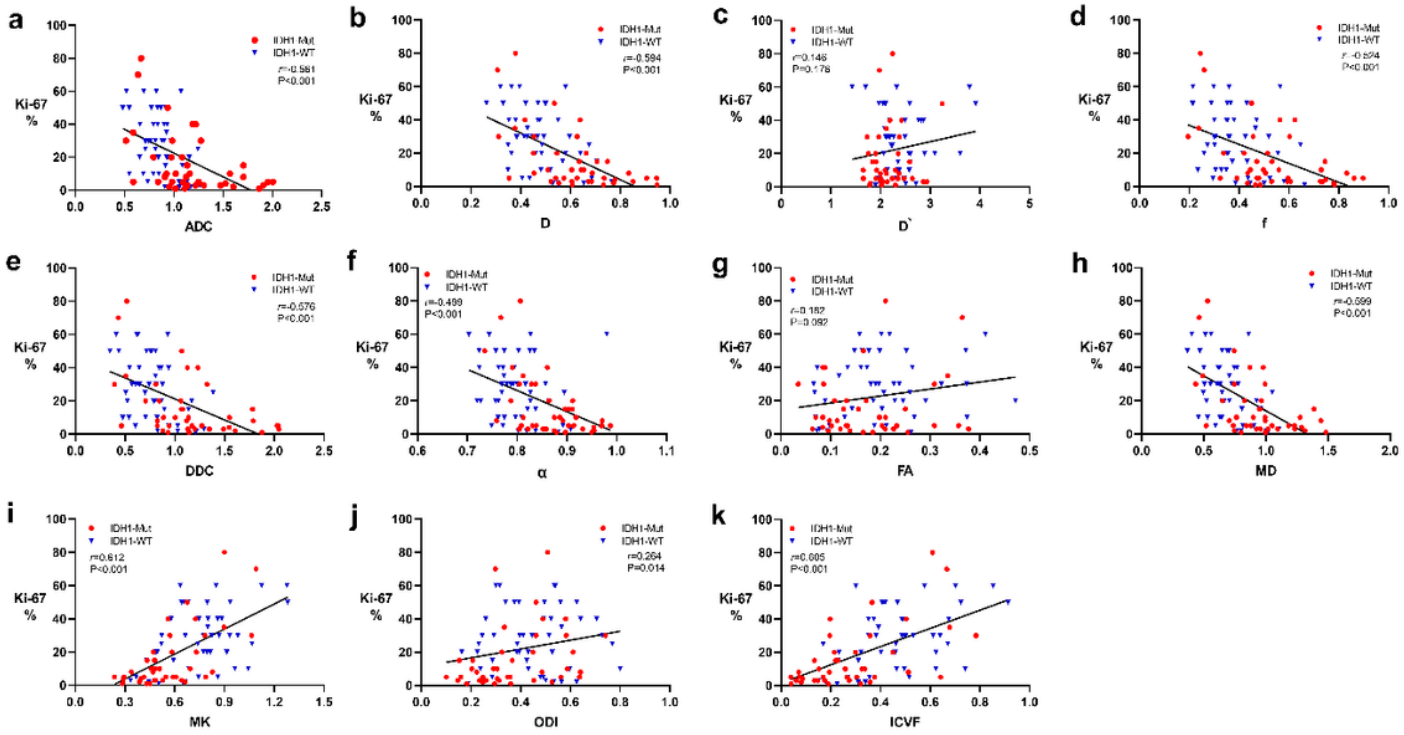

Figure 4

Scatter diagrams demonstrating the correlation between Ki-67 LI and each parameter. And r represents the Spearman correlation coefficient.

Supplementary Files

This is a list of supplementary files associated with this preprint. Click to download.

- Supplement.docx